

Vision-Language Alignment from Compressed Image Representations using 2D Gaussian Splatting

Yasmine Omri

yomri@stanford.edu

Connor Ding

czsding@stanford.edu

Tsachy Weissman*

tsachy@stanford.edu

Thierry Tambe*

ttambe@stanford.edu

*Equal advising

Department of Electrical Engineering, Stanford University

Abstract

Modern vision–language pipelines are driven by RGB vision encoders trained on massive image–text corpora. While these pipelines have enabled impressive zero-shot capabilities and strong transfer across tasks, they still inherit two structural inefficiencies from the pixel domain: (i) transmitting dense RGB images from edge devices to the cloud is energy-intensive and costly, and (ii) patch-based tokenization explodes sequence length, stressing attention budgets and context limits. We explore 2D Gaussian Splatting (2DGS) as an alternative visual substrate for alignment: a compact, spatially adaptive representation that parameterizes images by a set of colored anisotropic Gaussians. We develop a scalable 2DGS pipeline with structured initialization, luminance-aware pruning, and batched CUDA kernels, achieving over $90\times$ faster fitting and $\sim 97\%$ GPU utilization compared to prior implementations. We further adapt contrastive language-image pre-training (CLIP) to 2DGS by reusing a frozen RGB-based transformer backbone with a lightweight splat-aware input stem and a perceiver resampler, training only $\sim 7\%$ of the total parameters. On large DataComp subsets, GS encoders yield meaningful zero-shot ImageNet-1K performance while compressing inputs $3\text{--}20\times$ relative to pixels. While accuracy currently trails RGB encoders, our results establish 2DGS as a viable multimodal substrate, pinpoint architectural bottlenecks, and open a path toward representations that are both semantically powerful and transmission-efficient for edge–cloud learning.

1. Introduction

Expressive yet compact visual representations are central to progress in computer vision and multimodal learning. Recent advances in large multimodal models (LMMs), particularly visual language models (VLMs), have extended the reasoning capabilities of large language models beyond text, enabling impressive capabilities in visual question answering, image captioning, and cross-modal understanding. VLMs leverage a shared embedding space to enable joint reasoning over text, images, and other modalities [15, 16, 18–20, 31], as illustrated by Fig. 1a. Central to this paradigm are vision encoders that map raw images into sequences of visual tokens, semantically aligned with textual embeddings. The canonical pipeline starts from (often high-resolution) RGB images, which are patchified using a uniform grid and routinely projected into hundreds or thousands of tokens. These encoders typically adopt a vision transformer (ViT) backbone, trained via contrastive language–image pre-training (CLIP) on large image–caption datasets [26].

While effective, this paradigm suffers from two systemic inefficiencies. (1) Reliance on high-density RGB inputs imposes substantial data-transfer and energy costs in edge–cloud deployments: even when compressed into formats such as JPEG for transfer, visual data remains bandwidth-intensive and requires costly decoding before processing. (2) Patch-based tokenization causes a severe token explosion: whereas a text prompt may require only a few dozen tokens, vision encoders routinely emit hundreds or thousands per image, many of which are redundant. This redundancy inflates memory and compute costs

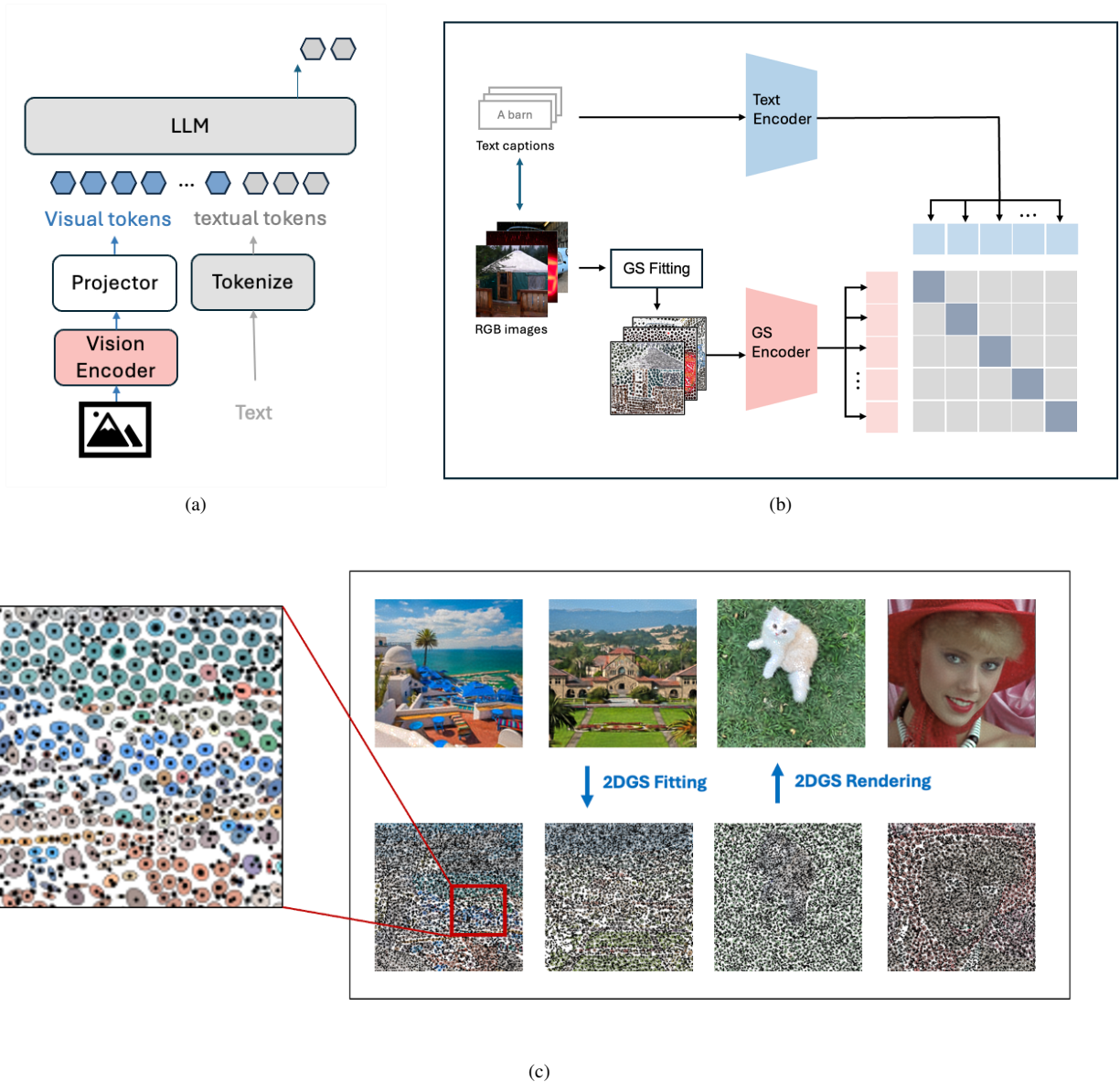


Figure 1. (a) Architecture of an autoregressive visual language model (VLM) (b) 2DGS adaptation of contrastive language-image pre-training (CLIP) (c) Illustration of 2D Gaussian Splatting (2DGS) for image fitting. Each image is represented as a sparse mixture of anisotropic Gaussians parameterized by position, covariance, and color. Summing contributions from all splats reconstructs the original image (with a minor and configurable degradation loss), enabling compact, spatially adaptive representations.

due to the quadratic scaling of attention, threatening the efficiency and sustainability of large-scale multimodal training and deployment.

We hypothesize that part of this inefficiency stems from a mismatch between human-centric visual formats and the needs of machine learning systems. RGB pixel arrays are tailored for human perception, with dense spatial correlations, but may include far more detail than models require. Unlike humans, who rely on full-resolution imagery, learning systems could benefit from more abstract representa-

tions that emphasize semantic and structural content while discarding perceptually oriented redundancy. This perspective raises a central research question: instead of transmitting perceptually complete images intended for human viewing, **can we design compact, semantically rich representations that preserve information critical for downstream learning while substantially reducing transmission overhead?**

This work presents the first large-scale exploration of 2D Gaussian Splatting (2DGS) as a visual representation

for vision–language alignment in multimodal systems. We ask a central question: **Can 2D Gaussian splats serve as an efficient and effective intermediate representation for generating text-aligned embeddings in contrastive vision–language models?** To address this, we explore both system-level optimizations for scalable 2DGS and architectural adaptations of contrastive language–image pre-training. Our contributions are two-fold:

- **Systems and Algorithmic Optimizations for Scalable 2DGS:** We introduce structured initialization, luminance-aware L1 pruning, and batched CUDA kernels, achieving over $90\times$ faster fitting (compared to existing baselines) and 97% GPU utilization. These optimizations make it feasible to generate millions of GS-encoded images for large-scale training.
- **Large-Scale CLIP Adaptation for Gaussian Splat Inputs:** We systematically adapt the CLIP framework to operate on 2DGS representations, via a novel GS stem, including Fourier positional encodings, log-scaled covariance representations, and a Perceiver Resampler pre-processing unit on GS inputs. Our approach leverages frozen RGB-based transformer backbones while introducing lightweight, splat-aware components, enabling efficient transfer learning from established vision encoders.

Our experimental evaluation on a 12.8M subset of DataComp [8] provides the first systematic study of GS-based vision encoders in zero-shot classification tasks, a widely used proxy for assessing vision–language alignment. While GS-based encoders currently trail RGB-based models in zero-shot accuracy, they demonstrate clear viability as compressed, transferable representations. Unlike RGB pipelines, which have benefited from years of architectural refinements and mature training recipes, 2DGS-based CLIP pipelines are in their early stages and poised for rapid improvement. We position this work not as an incremental patch-based encoder improvement, but as a first step toward a fundamentally different paradigm: building multimodal systems from inherently compact, adaptive representations rather than post-hoc compression of tokens.

2. Motivation and Related Work

The Edge-Cloud Data Transfer Challenge Modern multimodal pipelines increasingly depend on edge–cloud frameworks, where bandwidth-limited devices capture high-resolution visual data and transmit it to cloud-based vision encoders for semantic processing. Yet, this paradigm hides a critical inefficiency: transmitting dense RGB-based visual data remains energy-intensive, particularly for resource-constrained edge devices. Empirical studies indicate that mobile uplink transmission (the primary mode for edge devices) alone consumes approximately 0.1–0.2 kWh per GB, (as compared to ~ 0.03 kWh per GB for fixed broadband connections) [1]. At scale, this may translate to

tens of kilowatt-hours for just a few gigabytes of visual data. For instance, a single hour of 1080p video transmission consumes 0.38–0.68 kWh over mobile networks, energetically equivalent to powering a typical home for hours [9]. As such, the energy and infrastructure costs of naive RGB data transfer can quickly dominate operational budgets in real-world multimodal systems.

The Token Explosion Problem and the Increasing Strain on Context Lengths The second challenge emerges in downstream processing, where current vision encoders generate sequences of hundreds or thousands of tokens per image. For example, LLaVA-1.5 [19] emits 576 tokens for a 336×336 image, while LLaVA-NeXT [20] outputs over 2,880 tokens for 672×672 inputs, compared to about 20–50 tokens for a typical sentence in a text prompt. This visual information density creates severe computational bottlenecks, as self-attention scales quadratically with sequence length. To address this, recent work has focused on post-hoc token reduction. PruMerge [28] and VisionZip [33] implement text-agnostic selection strategies, with the former requiring LLM-level fine-tuning and the latter projector-level fine-tuning for optimal performance. ToMe [3] integrates token merging directly into encoder blocks via cosine-similarity–based selection. Progressive sparsification methods such as FastV [4] and SparseVLM [36] prune tokens layer by layer, guided by attention weights or cross-modal relevance. More recently, cluster-based aggregation [25] has shown that simple, finetuning-free grouping can outperform prior methods, with minimal loss in downstream performance. Strikingly, discarding up to 89% of visual tokens often has little effect on VQA benchmarks [7, 10, 12, 17, 21, 22, 29, 34], and in some cases even improves accuracy. Even naive strategies like spatial or random sampling perform competitively, highlighting the vast redundancy of current visual tokens.

While effective in reducing sequence length, these approaches remain constrained by patch-based tokenization; they are, in essence, band-aid solutions to an architectural inefficiency. The fact that most tokens can be discarded without harming performance underscores a deeper issue: today’s encoders may be producing large volumes of redundant, semantically shallow information. This not only inflates compute, but also raises a broader question: are patch-based encoders truly the right substrate for multimodal alignment? These findings suggest an opportunity to move beyond post-hoc pruning toward representations that are inherently compact, semantically expressive, and computationally efficient.

Compressed and Alternative Image Representations The limitation of post-hoc token reduction extends beyond compute efficiency. Such methods assume that optimal visual representations must originate from dense pixel

grids, and only later compress them. This paradigm overlooks the possibility that alternative input representations could be inherently more compact, expressive, and better aligned with the statistical patterns neural networks exploit.

Traditional codecs such as JPEG achieve high compression ratios but yield representations that lack interpretability for learning systems, though some work has explored making compressed formats more machine-friendly. Implicit neural representations (INRs) instead encode signals as continuous functions parameterized by neural networks, achieving high fidelity in compression and reconstruction [30]. Recent studies have even treated INR parameters as input embeddings for downstream tasks, with promising results [2, 6]. However, INRs remain computationally costly to optimize and are ill-suited for large-scale training pipelines.

A recent alternative is 2D Gaussian Splatting (2DGS): a 2D adaptation [35] of 3D Gaussian Splatting for real-time radiance field rendering [14]. 2DGS parameterizes images as sparse mixtures of anisotropic Gaussians, each defined by spatial position, covariance, and color. Unlike uniform patch grids, 2DGS adapts its representational density to local image complexity. Early studies show state-of-the-art image fitting with orders-of-magnitude faster encoding than INRs, making it far more practical for large-scale use. Preliminary work also suggests its viability as both a codec and a feature representation for small-scale classification tasks.

Yet, the potential of 2DGS as a learnable substrate for large-scale multimodal alignment remains unexplored. Meeting this challenge requires representations that capture not only visual fidelity but also semantic alignment with text. We argue that the compactness and adaptivity of 2DGS make it a particularly promising candidate for efficient, semantically meaningful visual embeddings in multimodal systems.

3. Preliminaries

3.1. 2D Gaussian Splatting as a Compressor

Building on 3D Gaussian Splatting (3DGS) for real-time novel-view synthesis [14], [35] introduced GaussianImage, adapting the concept for single-image compression. Instead of heavy 3D Gaussians requiring tens of parameters, GaussianImage uses compact 2D Gaussians parameterized by only eight values: 2D position, anisotropic covariance, and color, as illustrated by Fig. 1c. Images are reconstructed by summing contributions from all Gaussians, following Equation 1.

$$\hat{I}(x, y; \{\boldsymbol{\mu}_i, \boldsymbol{\Sigma}_i, \mathbf{c}_i\}_{i=1}^n) = \sum_{i=1}^n \mathbf{c}_i \exp \left\{ -\frac{1}{2} \left(\begin{bmatrix} x \\ y \end{bmatrix} - \boldsymbol{\mu}_i \right)^\top \boldsymbol{\Sigma}_i^{-1} \left(\begin{bmatrix} x \\ y \end{bmatrix} - \boldsymbol{\mu}_i \right) \right\}, \quad (1)$$

where $\hat{I}(x, y)$ is the predicted image intensity at pixel (x, y) , $\boldsymbol{\mu}_i \in \mathbb{R}^2$ is the Gaussian center, $\boldsymbol{\Sigma}_i \in \mathbb{R}^{2 \times 2}$ its covariance (often expressed by three free parameters), and \mathbf{c}_i its color.

2D Gaussian Splatting eliminates the need for depth sorting, enabling extremely fast rendering (1,500–2,000 FPS, or equivalently over 3X the decoding speed of JPEG), substantial memory savings, and $\sim 5 \times$ faster training compared to implicit neural representations (INRs) such as WIRE [27] or I-NGP [24] [35].

For further compression, GaussianImage employs a quantization pipeline (16-bit floats for positions, 6-bit integer covariance quantization, residual vector quantization for color, and partial bits-back coding). This achieves rate–distortion performance comparable to INR-based codecs while offering orders-of-magnitude faster decoding [35]. Following this, [37] proposed LIG (Large Images are Gaussians), a hierarchical two-level scheme that first fits low-frequency content and then refines high-frequency details, significantly improving scalability to ultra-high-resolution images. Extending to video, GSVC [32] predicts Gaussians sequentially across frames, prunes low-impact ones, adds new splats as needed, and reinitializes at keyframes, achieving AV1/VVC-level rate–distortion performance while decoding 1080p video at 1,500 FPS [32].

3.2. 2D Gaussian Splatting as a Learnable Representation

Beyond compression, 2DGS has been explored as a learnable substrate for vision tasks. GViT [11] replaces pixel patches with hundreds of Gaussians, and jointly optimizes them with a Vision Transformer. A differentiable renderer enforces image reconstruction, while classification gradients push Gaussians toward discriminative regions, yielding a compact, interpretable representation that matches ViT-B performance on ImageNet-1K (76.9% top-1) supervised classification. [5] proposes GaussianToken, which encodes images as Gaussians with continuous spatial parameters and feature coefficients, quantized via a VQ codebook and concatenated with spatial attributes. This hybrid token design improves reconstruction fidelity over VQ-VAE tokenizers.

Yet, existing efforts remain limited to small-scale settings. The role of 2DGS as a foundation for large-scale multimodal alignment, where representations must balance

compactness, semantic richness, and learnability, has not been systematically investigated. Our work addresses this gap, providing the first large-scale study of 2DGS within vision–language pre-training.

In the context of our work, the key takeaway is that 2DGS provides a compact, spatially adaptive, and computationally efficient image representation. Rather than using 2DGS solely as a codec, we investigate its role as a learnable substrate for multimodal alignment, asking whether its promising properties can support large-scale vision–language pre-training.

3.3. Contrastive Language-Image Pre-training (CLIP)

Vision–language alignment is commonly achieved through Contrastive Language–Image Pre-Training (CLIP), which trains a dual-encoder architecture on image–caption pairs. A text encoder and a vision encoder are optimized jointly so that embeddings of aligned pairs are pulled closer, and mismatched pairs pushed apart under a contrastive loss [26]. CLIP has become the standard paradigm, demonstrating strong performance across a wide range of downstream multimodal tasks. The CLIP framework spans a family of models from lightweight 25M-parameter encoders to larger 300M+ parameter variants such as ViT-L/14, all of which require hundreds of millions of training samples and significant compute to reach high-quality alignment.

In this work, we retain the CLIP training recipe but investigate whether 2D Gaussian Splatting can serve as an alternative visual substrate. Using the OpenCLIP implementation [23], we directly compare RGB- and 2DGS-based encoders under identical training conditions, isolating the effect of the representation itself. Our approach further reuses frozen RGB-pretrained backbones with lightweight splat-aware input modules, enabling efficient adaptation while substantially reducing trainable parameters.

4. Optimizations for Efficient and Scalable 2D Gaussian Splatting

4.1. Challenges

Scaling 2D Gaussian Splatting (2DGS) for vision–language alignment faces three main challenges. First, without efficient batching, fitting a single image requires multiple forward and backward passes through a differentiable renderer, taking several seconds and making large-scale training impractical. Second, the current ecosystem lacks maturity: open implementations such as GaussianImage lack batch optimization and exhibit poor GPU utilization, further limiting throughput. Finally, achieving useful compression requires careful trade-offs: reducing the number of Gaussians lowers cost, but naïve pruning can harm perceptual quality and discard semantically important information. Together,

these issues restrict the applicability of 2DGS in multimodal pipelines and motivate our system- and algorithm-level optimizations.

4.2. Specialized CUDA Kernels for Scalable 2DGS

Our implementation builds on the open-source Gaussian-Image codebase [35], which first introduced 2D Gaussian Splatting for high-speed image representation. Subsequent work by [37] streamlined this design, restructuring the kernels and data flow specifically for 2D operations and thereby yielding a cleaner, more efficient foundation for image representation.

This codebase is structured as follows: the forward pass is decomposed into two phases: (1) a projection stage, wherein each Gaussian primitive is projected onto a 2D grid of pixels. The grid is tiled across thread blocks, where each block corresponds to a 2D tile of the output image. Within a block, individual threads are assigned to pixels, computing Gaussian weights and contributions in parallel. This design ensures that Gaussian evaluation is parallelized across both the spatial dimension (pixels) and across different Gaussians, and (2) a rasterization stage, wherein the projected Gaussians are accumulated to produce the final output image at each iteration. This stage handles blending and weighting of Gaussians for each pixel. Unlike projection, where computation is Gaussian-centric, rasterization is pixel-centric, with threads accumulating contributions into shared output buffers. The backward pass is handled by a dedicated kernel that computes gradients of the loss with respect to Gaussian parameters (positions, covariances, colors). Workload partitioning is inverted relative to the forward pass: each block is assigned to a 2D tile of the input grid, and threads within the block compute pixel-level derivatives. This tiling strategy balances workload across warps and ensures efficient coalesced memory access when accumulating gradients.

We extend the implementation with batched input support by introducing several key modifications:

- Batch-aware memory layout: Indexing and memory access patterns were modified to include the batch dimension, allowing multiple images to be processed concurrently.
- Additional synchronization threads were inserted at critical points to ensure that all threads complete their batch-local computations before proceeding, preventing race conditions when accumulating results.
- Shared memory usage: Shared memory, already used in the original codebase for intermediate accumulation, was expanded to cache per-batch partial results. This reduces the frequency of global memory accesses and improves overall throughput.

With these modifications, the codebase now supports high-

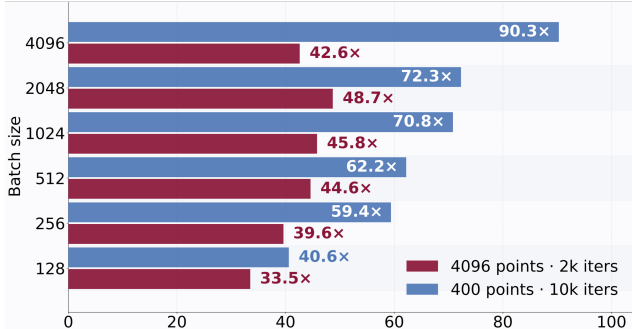


Figure 2. Speedup results achieved by our CUDA kernels compared to the [37] baseline, following our batch-aware implementation. Speedups are presented for various batch sizes and Gaussian counts for image resolutions of 224x224. For a batch size of 4096 and 400 Gaussian points per image, we observe a 90.3X speedup compared to the baseline.

speed processing of thousands of inputs concurrently, making the implementation suitable for large-scale training pipelines. Notably, our enhanced codebase enables up to 90X speedup in fitting time compared to the baseline open-sourced codebase by [37] with 97% GPU utilization, profiled using NVIDIA Nsight Compute. Fig. 2 presents speedup results for various batch sizes and gaussian counts. Our optimized 2DGS pipeline, including both our algorithmic and system-level optimizations will soon be open-sourced to enable further explorations of 2DGS.

4.3. Structured Initialization



Figure 3. Visualization of reconstruction results for random vs. structured initialization (Ours) for 2DGS fitting for a fixed number of iterations (3000): structured initialization accelerates convergence and achieves higher perceptual quality than random initialization. This is consistent across various compression ratios (ie, numbers of Gaussian points per image) especially for more aggressive compression ratios.

Traditional 2D Gaussian splatting approaches follow the conventions established in 3D Gaussian splatting, where

random initialization of Gaussian parameters is the standard practice. In 3D scene reconstruction, this random initialization strategy is well-motivated, because the underlying 3D geometry is unknown a priori, and points must be discovered through optimization. The 3D case deals with sparse, incomplete observations of a scene from multiple viewpoints, making a structured initialization impractical without prior geometric knowledge. However, the 2D image case presents a fundamentally different scenario where we can leverage the pixel-level prior information available in the input image. Unlike 3D reconstruction where we must infer spatial structure, 2D images provide direct access to spatial organization and color information at every pixel location. Our structured initialization strategy exploits this pixel prior through three key components:

- **Position Initialization:** Rather than randomly sampling Gaussian centers, we initialize the x,y coordinates of each Gaussian following a uniformly distributed grid pattern across the image dimensions. This grid-based approach maximizes spatial coverage, ensuring that each region receives appropriate representational capacity from the start of optimization.
- **Covariance Initialization:** Each Gaussian starts with an isotropic covariance, corresponding to the largest circle that can be fitted into the grid.
- **Color:** RGB values are initialized as the average color RGB value of all pixels in the grid. This color inheritance provides a strong starting point for optimization, as each Gaussian begins with a color value that is already locally appropriate for its spatial region.

As illustrated by Fig. 3, this design provides strong priors that accelerate optimization. With 4,900 Gaussians, structured initialization achieves 33.07 PSNR versus 21.09 for random initialization. Even at 400 Gaussians, it maintains 25.75 PSNR versus 18.48, demonstrating both faster convergence and higher asymptotic perceptual quality.

4.4. Adaptive Pruning through L1 Regularization and Luminance Thresholding

Achieving optimal compression while preserving semantic information requires intelligent removal of redundant Gaussian primitives during optimization. Our adaptive pruning strategy combines L1 regularization with luminance-based thresholding to identify and eliminate Gaussians that contribute minimally to overall reconstruction quality.

- **L1 Regularization Framework:** We incorporate L1 penalty terms on the color channels of the Gaussian points during fitting to naturally encourage sparsity during optimization. This regularization framework allows the model to automatically identify low-contribution Gaussians by driving their parameters toward zero, making them candidates for removal without explicit supervision.
- **Information-Density Aware Pruning:** Our pruning

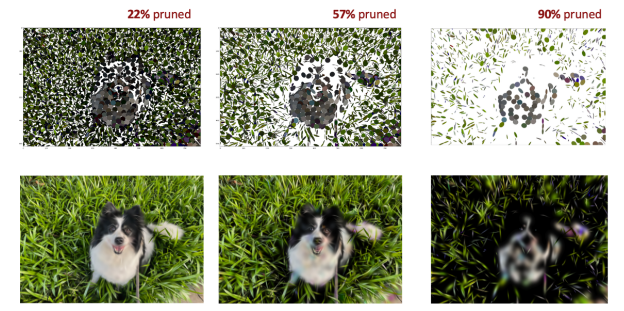


Figure 4. Visualization of our adaptive pruning configurability: the pruning ratio is adaptive and configurable through both the luminance threshold and the L1 regularization hyperparameter. While very high pruning ratios may result in significant perceptual quality loss, we observe that conservative pruning ratios (as high as $\sim 20\%$, recommended for human perception) result in barely noticeable degradation loss, and pruning ratios of $\sim 50\%$ allow an acceptable reconstruction quality while halving the number of Gaussian points.

strategy, illustrated by Fig. 4, operates based on the principle that not all image regions contribute equally to vision-language understanding. We dynamically assess each Gaussian’s contribution to overall reconstruction quality and prioritize removal of those in regions with low information density for downstream multimodal tasks. Gaussians located in low-luminance regions often correspond to areas with minimal visual information. Our luminance-based thresholding mechanism identifies these regions and marks associated Gaussians for removal, reducing the final number of Gaussian points, while preserving semantically important visual content.

5. Vision-Language Alignment at Scale from 2DGS Representations

5.1. Methodology and Experimental Setup

Transfer Learning from RGB Backbones

We first train an RGB baseline CLIP model, using a ViT-B-16 and its corresponding text encoder. For more scalable experiments, we reduce the model width from 716 down to 512 which results in 38M weights for the vision encoder (instead of 88M, though comparable performance is maintained on our data subset). All models are trained using the OpenCLIP framework with a standardized configuration: learning rate of $1e-3$, 32 training epochs, local batch size of 256, cosine learning rate scheduler, and weight decay of 0.2. We utilize a 12.8M image-text dataset from DataComp for training, providing a substantial yet manageable scale for our comparative analysis [8]. We conduct our experiments on the Marlowe data center using a single node equipped with 8 H100 GPUs [13].

To assess the quality of vision encoder alignment and generalization capabilities, we track zero-shot accuracy on the ImageNet-1K validation set with evaluation frequency of one epoch. After training our conventional RGB-based CLIP model, we select the checkpoint corresponding to the highest validation accuracy achieved during training, defined as the zero-shot top-1 classification accuracy achieved by the vision encoder on ImageNet-1K validation set.

We leverage this optimal RGB checkpoint to perform lightweight transfer learning to the 2DGS domain. In particular, we craft a 2DGS-based vision encoder that shares the same transformer backbone and transformer weights as the RGB vision encoder. We tailor the encoder stem “GS stem” to the unique properties and structure of 2DGS data.

For training, we freeze the RGB text encoder, and all of the transformer backbone (initialized with the RGB weights) apart from the first 2 layers. We train only the remaining 7% of the model parameters for 6 epochs to establish alignment between standard RGB inputs and text through a tailored adaptation stem. This is illustrated by Fig. 5. We use the base learning rate of $1e-3$ for the GS stem, and a small learning rate equal to $0.1 \times$ the base LR for the unfrozen first 2 layers of the transformer, as well as the post transformer normalization and projection. This efficient approach leverages existing representations while minimizing computational overhead.

Our GS encoder processes 2DGS representations through several key components. In particular, the GS Stem handles the initial processing of raw 2D Gaussian splat parameters through a sophisticated multi-stage pipeline designed to extract meaningful features from the compact Gaussian representation:

- **Fourier Encoding:** Each 2D Gaussian splat is characterized by parameters including 2D position (x, y), covariance matrix elements, and RGB color values. The positional components undergo Fourier feature encoding, which maps the continuous 2D coordinates into a higher-dimensional space using sinusoidal functions at multiple frequencies. This encoding enables the model to capture both coarse and fine-grained spatial relationships between Gaussian primitives, essential for understanding spatial structure in the splat representation.
- **Gated Sigmoid Linear Layer:** A gating mechanism applies element-wise multiplication between the linearly projected features and a sigmoid-activated gating vector learned from the same input. This allows the model to selectively emphasize or suppress different aspects of each Gaussian splat based on its parameters, enabling adaptive feature selection that can focus on the most informative splats for a given image.
- **Z-score Normalization:** Layer-wise normalization standardizes the feature distributions by subtracting a subset-wide mean and dividing by the standard deviation across

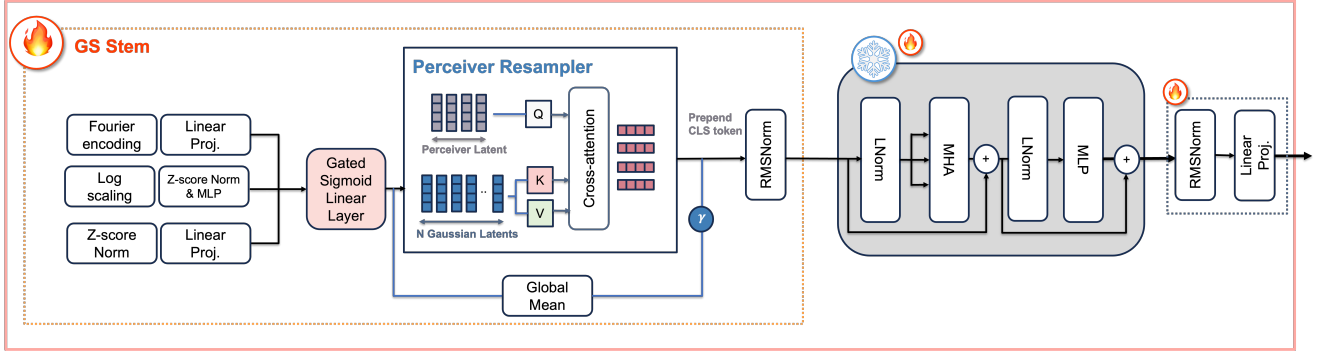


Figure 5. Architecture of our 2DGS-adapted CLIP pipeline: a splat-aware stem embeds a configurable number of Gaussian points using Fourier features, log scaling, normalization layers, and projections. These embeddings are processed by a majoritarily frozen RGB-pretrained transformer.

the feature dimension. This ensures stable training dynamics and helps the model handle varying numbers and scales of Gaussian splats across different images.

The processed Gaussian features then pass through the Perceiver Resampler, which employs cross-attention between a learned set of query tokens and the variable-length sequence of Gaussian latent representations. This cross-attention mechanism iteratively refines a fixed number of output tokens (196: equal to the number of tokens outputted by the RGB ViT-B-16 baseline, or 98 corresponding to a 50% reduction in output tokens) by attending to the most relevant Gaussian features, effectively downsampling the potentially large number of input splats to a manageable representation size. Global Mean pooling provides additional spatial aggregation, computing average statistics across all processed Gaussian features before the final integration with the frozen CLIP transformer backbone.

This architecture enables end-to-end learning from 2DGS representations while leveraging the robust feature extraction capabilities of pretrained vision-language models.

5.2. Results

Our preliminary zero-shot classification results demonstrate promising progress in adapting vision-language models to 2DGS representations, revealing several encouraging findings that highlight the potential of this approach. As illustrated by Fig. 6, Our 2DGS models achieve meaningful zero-shot performance with top-1 accuracies of 13-15% and top-5 accuracies of 30-35%, compared to the upper-bound RGB teacher model top-1 accuracy of 18.5% and top-5 accuracy of 40%. This establishes a foundation for future development while offering substantial input compression advantages (3-23.5x) over traditional pixel-based representations. The results showcase consistency across compression ratios from 3x to 12x with more pronounced degradation for compression ratios exceeding 20x, compared to the

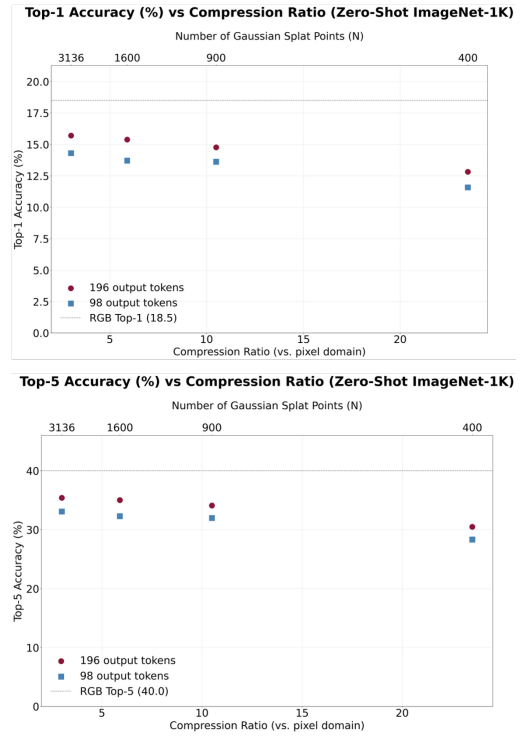


Figure 6. Zero-shot ImageNet-1K results for 2DGS-based encoders. Models achieve 13–15% top-1 and 30–35% top-5 accuracy while compressing inputs by 3–20x compared to pixels. Accuracy remains stable across splat counts and compression ratios of up to 12x, with the 196-token setting outperforming 98 tokens, highlighting both robustness and the benefit of greater representational capacity.

pixel domain. These ratios are calculated using float16 precision for all Gaussian splat parameters, with the potential for even more dramatic compression gains when employing the quantization techniques proposed in the Gaussian-Image work [35]. Notably, performance trends remain sta-

ble across varying numbers of Gaussian splat points (400 to 3136), demonstrating the robustness of our approach and suggesting that the Perceiver Resampler successfully captures essential visual information even from sparse representations. The consistent advantage of the 196-token configuration over the 98-token variant confirms that increased representational capacity enhances alignment quality, while the overall stability of results across different splat densities indicates that our architecture effectively processes the unique characteristics of Gaussian representations, with remaining room for improvement. These findings establish 2DGS as a viable alternative visual encoding for multimodal learning, with clear pathways for closing the remaining performance gap with RGB encoders.

5.3. Discussion

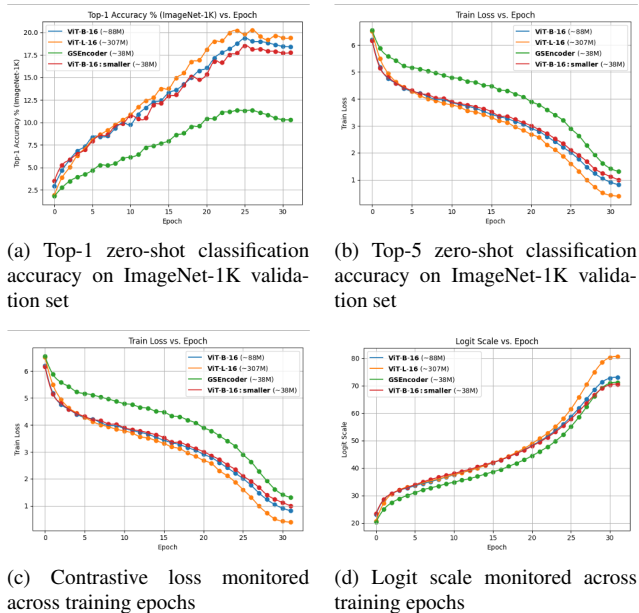


Figure 7. Training 2DGS encoders from scratch performs significantly worse than our parameter-efficient adaptation approach. These results highlight the current difficulty of pre-training from scratch directly from Gaussian inputs.

Our results highlight both the promise and current limitations of 2DGS for vision–language alignment. Accuracy on ImageNet-1K lags behind RGB encoders by roughly 3–5 points under the same training setup, underscoring the gap that remains. At the same time, stability across compression ratios and splat densities suggests that 2DGS retains semantically useful information even in highly compact form.

We also experimented with training 2DGS encoders from scratch, which so far perform worse than our parameter-efficient adaptation approach, as seen in Fig. 7. Nonetheless, these trials provide insight into which architectural components and training procedures may be critical

for models that learn directly from Gaussian inputs. Given the relative novelty of 2DGS in machine learning, the design space for architectures and recipes tailored to this representation remains largely unexplored.

Looking ahead, progress will likely rest on modeling innovations (e.g., encoders explicitly structured around splat geometry). We see this work as a first step toward establishing 2DGS as a multimodal substrate, compact and transmission-efficient, while opening concrete directions for closing the accuracy gap with RGB pipelines.

6. Conclusion

In this work, we presented the first large-scale study of 2D Gaussian Splatting (2DGS) as a visual representation for contrastive vision–language alignment. Our contributions span both systems and modeling. On the systems side, we introduced structured initialization, luminance-aware pruning with L1 regularization, and batched CUDA kernels, yielding over $90\times$ faster fitting with $\sim 97\%$ GPU utilization. On the modeling side, we adapted CLIP to 2DGS inputs by adding a splat-aware input stem and Perceiver-style resampler to a frozen RGB-pretrained transformer, updating only 7% of parameters.

Empirically, 2DGS-based encoders achieve 13–15% zero-shot ImageNet-1K top-1 accuracy under $3\text{--}23.5\times$ compression relative to pixels, with stable behavior across splat counts. These results suggest that much of the semantic signal required for alignment can be retained in a compact, spatially adaptive representation, supporting the case for visual inputs that are better matched to both compute and communication constraints than dense RGB.

Nonetheless, limitations remain. Accuracy currently lags RGB baselines by a few points, reflecting that early-stage training recipes, positional encodings, and resampling strategies are not yet optimally tuned for splat inputs. Our current pipeline also omits codec-side quantization (e.g., covariance or codebook quantization) during alignment.

We see several promising directions for advancing 2DGS-based multimodal learning:

1. **Joint representation–alignment training** with novel model architectures better suited for 2DGS inputs;
2. **Video and streaming extensions** that model and learn from splats across time; and
3. **End-to-end edge–cloud evaluation**, measuring not only accuracy but also energy and latency benefits of transmission-efficient representations.

We position this work as a first step toward representation-first multimodal learning, where compact, structured inputs such as 2DGS become native substrates for alignment, moving beyond post-hoc pruning toward fundamentally more efficient and adaptive vision–language systems.

Acknowledgments

We thank the staff of the Stanford Marlowe computing cluster, in particular Kurt Stine and Craig Kapfer, for their continued support during our project. We are also grateful to NVIDIA solutions architects Zoe Ryan and Amanda Butler for their assistance with large-scale profiling and speedup. Finally, we thank Yuhui Zhang, Kedar Tatwawadi, Suresh Nambi, Ludwig Schmidt, Fernando Mujica, Mert Pelanci, and Marcel Rod for their insightful feedback and discussions.

References

- [1] Eu ict impact study on energy intensity of mobile vs fixed data. Energy consumption estimates: 0.14 kWh/GB (mobile) vs 0.03 kWh/GB (fixed broadband), 2020. As reported in Scope3/EU ICT impact study via methodology.scope3.com. 3
- [2] Matthias Bauer, Emilien Dupont, Andy Brock, Dan Rosenbaum, Jonathan Richard Schwarz, and Hyunjik Kim. Spatial functa: Scaling functa to imagenet classification and generation. *arXiv preprint arXiv:2302.03130*, 2023. 4
- [3] Daniel Bolya, Cheng-Yang Fu, Xiaoliang Dai, Peizhao Zhang, Christoph Feichtenhofer, and Judy Hoffman. Token merging: Your vit but faster. *arXiv preprint arXiv:2210.09461*, 2022. 3
- [4] Liang Chen, Haozhe Zhao, Tianyu Liu, Shuai Bai, Junyang Lin, Chang Zhou, and Baobao Chang. An image is worth 1/2 tokens after layer 2: Plug-and-play inference acceleration for large vision-language models. *arXiv preprint arXiv:2403.06764*, 2024. 3
- [5] Jiajun Dong, Chengkun Wang, Wenzhao Zheng, Lei Chen, Jiwen Lu, and Yansong Tang. Gaussiantoken: An effective image tokenizer with 2d gaussian splatting. *arXiv preprint arXiv:2501.15619*, 2025. 4
- [6] Emilien Dupont, Hyunjik Kim, S. M. Ali Eslami, Danilo Rezende, and Dan Rosenbaum. From data to functa: Your data point is a function and you can treat it like one. In *International Conference on Machine Learning (ICML)*, 2022. 4
- [7] Chaoyou Fu, Peixian Chen, Yunhang Shen, Yulei Qin, Mengdan Zhang, Xu Lin, Jinrui Yang, Xiawu Zheng, Ke Li, Xing Sun, Yunsheng Wu, and Rongrong Ji. Mme: A comprehensive evaluation benchmark for multimodal large language models. *arXiv preprint arXiv:2306.13394*, 2023. 3
- [8] Samir Yitzhak Gadre, Gabriel Ilharco, Alex Fang, Jonathan Hayase, Georgios Smyrnis, Thao Nguyen, Ryan Marten, Mitchell Wortsman, Dhruva Ghosh, Jieyu Zhang, Eyal Orgad, Rahim Entezari, Giannis Daras, Sarah Pratt, Vivek Ramanujan, Yonatan Bitton, Kalyani Marathe, Stephen Mussmann, Richard Vencu, Mehdi Cherti, Ranjay Krishna, Pang Wei Koh, Olga Saukh, Alexander Ratner, Shuran Song, Hannaneh Hajishirzi, Ali Farhadi, Romain Beaumont, Sewoong Oh, Alex Dimakis, Jenia Jitsev, Yair Carmon, Vaishaal Shankar, and Ludwig Schmidt. Datacomp: In search of the next generation of multimodal datasets. In *Advances in Neural Information Processing Systems (NeurIPS)*, 2023. 3, 7
- [9] GSMA Intelligence. Mobile networks use 0.13 kwh per gb of data (2021). Digital 2025 mobile data consumption trends report, 2025. Energy consumption for mobile data transfer. 3
- [10] Danna Gurari, Qing Li, Abigale J. Stangl, Anhong Guo, Chi Lin, Kristen Grauman, Jiebo Luo, and Jeffrey P. Bigham. Vizwiz grand challenge: Answering visual questions from blind people. In *Proceedings of the IEEE Conference on Computer Vision and Pattern Recognition (CVPR)*, 2018. 3
- [11] Jefferson Hernandez, Ruozhen He, Guha Balakrishnan, Alexander C. Berg, and Vicente Ordonez. Gvit: Representing images as gaussians for visual recognition. *arXiv preprint arXiv:2506.23532*, 2025. 4
- [12] Drew A. Hudson and Christopher D. Manning. Gqa: A new dataset for real-world visual reasoning and compositional question answering. In *Proceedings of the IEEE/CVF Conference on Computer Vision and Pattern Recognition (CVPR)*, 2019. 3
- [13] C. Kapfer, K. Stine, B. Narasimhan, C. Mentzel, and E. Candès. Marlowe: Stanford’s gpu-based computational instrument (0.1). Zenodo, 2025. 7
- [14] Bernhard Kerbl, Georgios Kopanas, Thomas Leimkuehler, and George Drettakis. 3d gaussian splatting for real-time radiance field rendering. *arXiv preprint arXiv:2308.04079*, 2023. 4
- [15] Bo Li, Yuanhan Zhang, et al. Llava-onevision: Easy visual task transfer. *arXiv preprint arXiv:2408.03326*, 2024. 1
- [16] Junnan Li, Dongxu Li, Silvio Savarese, and Steven Hoi. Blip-2: Bootstrapping language-image pre-training with frozen image encoders and large language models. *arXiv preprint arXiv:2301.12597*, 2023. 1
- [17] Yifan Li, Yifan Du, Kun Zhou, Jinpeng Wang, Wayne Xin Zhao, and Ji-Rong Wen. Evaluating object hallucination in large vision-language models. In *Proceedings of the Conference on Empirical Methods in Natural Language Processing (EMNLP)*, 2023. 3
- [18] Ji Lin, Hongxu Yin, Wei Ping, Yao Lu, Pavlo Molchanov, Andrew Tao, Huizi Mao, Jan Kautz, Mohammad Shoeybi, and Song Han. Vila: On pre-training for visual language models. In *Proceedings of the IEEE/CVF Conference on Computer Vision and Pattern Recognition (CVPR)*, 2024. 1
- [19] Haotian Liu and Chunyuan Li. Improved baselines with visual instruction tuning. *arXiv preprint arXiv:2310.03744*, 2023. 3
- [20] Haotian Liu, Chunyuan Li, et al. Llava next: Improved reasoning, ocr, and world knowledge. <https://llava-vl.github.io/blog/2024-01-30-llava-next/>, 2024. 1, 3
- [21] Y Liu et al. Mmbench: Is your multi-modal model an all-around player? In *Proceedings of the European Conference on Computer Vision (ECCV)*, 2024. Oral presentation. 3
- [22] Pan Lu, Swaroop Mishra, Tony Xia, Liang Qiu, Kai-Wei Chang, Song-Chun Zhu, Oyvind Tafjord, Peter Clark, and Ashwin Kalyan. Learn to explain: Multimodal reasoning via thought chains for science question answering. In *Advances in Neural Information Processing Systems (NeurIPS)*, 2022. 3

- [23] mlfoundations. open_clip: An open source implementation of clip. Zenodo, 2021. 5
- [24] Thomas Müller, Alex Evans, Christoph Schied, and Alexander Keller. Instant neural graphics primitives with a multiresolution hash encoding. *ACM Transactions on Graphics*, 41(4):1–15, 2022. 4
- [25] Yasmine Omri, Parth Shroff, and Thierry Tambe. Token sequence compression for efficient multimodal computing. *arXiv preprint arXiv:2504.17892*, 2025. 3
- [26] Alec Radford, Jong Wook Kim, Chris Hallacy, Aditya Ramesh, Gabriel Goh, Sandhini Agarwal, Girish Sastry, Amanda Askell, Pamela Mishkin, Jack Clark, Gretchen Krueger, and Ilya Sutskever. Learning transferable visual models from natural language supervision. *arXiv preprint arXiv:2103.00020*, 2021. 1, 5
- [27] Vishwanath Saragadam, Daniel LeJeune, Jasper Tan, Guha Balakrishnan, Ashok Veeraraghavan, and Richard G. Baraniuk. Wire: Wavelet implicit neural representations, 2023. 4
- [28] Yuzhang Shang, Mu Cai, Bingxin Xu, Yong Jae Lee, and Yan Yan. Llava-prumerge: Adaptive token reduction for efficient large multimodal models. *arXiv preprint arXiv:2403.15388*, 2024. 3
- [29] Amanpreet Singh and etc. Li. Towards vqa models that can read. In *Proceedings of the IEEE/CVF Conference on Computer Vision and Pattern Recognition (CVPR)*, 2019. 3
- [30] Vincent Sitzmann, Julien N.P. Martel, Alexander W. Bergman, David B. Lindell, and Gordon Wetzstein. Implicit neural representations with periodic activation functions. In *Conference on Neural Information Processing Systems (NeurIPS)*, 2020. 4
- [31] Adept AI Team. Fuyu-8b: A multimodal architecture for ai agents. <https://www.adept.ai/blog/fuyu-8b>, 2023. 1
- [32] Longan Wang, Yuang Shi, and Wei Tsang Ooi. Gsvc: Efficient video representation and compression through 2d gaussian splatting. *arXiv preprint arXiv:2501.12060*, 2025. 4
- [33] Senqiao Yang, Yukang Chen, Zhuotao Tian, Chengyao Wang, Jingyao Li, Bei Yu, and Jiaya Jia. Visionzip: Longer is better but not necessary in vision language models. *arXiv preprint arXiv:2412.04467*, 2024. 3
- [34] et al. Yu. Mm-vet: A benchmark to evaluate large multimodal models for integrated capabilities. *arXiv preprint arXiv:2408.00765*, 2024. 3
- [35] Xinjie Zhang, Xingtong Ge, Tongda Xu, Dailan He, Yan Wang, Hongwei Qin, Guo Lu, Jing Geng, and Jun Zhang. Gaussianimage: 1000 fps image representation and compression by 2d gaussian splatting. In *Proceedings of the European Conference on Computer Vision (ECCV)*, 2024. 4, 5, 8
- [36] Yuan Zhang, Chun-Kai Fan, Junpeng Ma, Wenzhao Zheng, Tao Huang, Kuan Cheng, Denis Gudovskiy, Tomoyuki Okuno, Yohei Nakata, Kurt Keutzer, et al. Sparsevlm: Visual token sparsification for efficient vision-language model inference. In *Proceedings of the International Conference on Machine Learning (ICML)*, 2025. 3
- [37] Lingting Zhu, Guying Lin, Jinnan Chen, Xinjie Zhang, Zhenchao Jin, Zhao Wang, and Lequan Yu. Large images are gaussians: High-quality large image representation with levels of 2d gaussian splatting. *arXiv preprint arXiv:2502.09039*, 2025. 4, 5, 6